Molecular Plant Pathology

WILEY

Molecular Plant Pathology

ORIGINAL ARTICLE OPEN ACCESS

Wheat *TaNADPO* Promotes Spot Blotch Resistance

Meng Yuan[1] | Qingdong Zeng[2] | Lei Hua[3] | Shisheng Chen[3] | Jianhui Wu[2] | Shuqing Zhao[1,2] | Mengyu Li[1,3] | Xiaopeng Ren[1] | Linfei Ma[1] | Zihan Liu[1] | Kaixuan Wang[1] | Manli Sun[1] | Hongfei Yan[1] | Zhensheng Kang[2] | Dejun Han[2] | Xiaodong Wang[1]

[1]State Key Laboratory of North China Crop Improvement and Regulation, College of Plant Protection, Hebei Agricultural University, Baoding, China | [2]State Key Laboratory of Crop Stress Resistance and High-Efficiency Production, College of Plant Protection, Northwest A&F University, Xianyang, China | [3]National Key Laboratory of Wheat Improvement, Shandong Laboratory of Advanced Agricultural Sciences in Weifang, Peking University Institute of Advanced Agricultural Sciences, Shandong, China

Correspondence: Dejun Han (handj@nwafu.edu.cn) | Xiaodong Wang (zhbwxd@hebau.edu.cn)

Received: 6 January 2025 | **Revised:** 10 May 2025 | **Accepted:** 19 May 2025

Funding: This work was supported by the National Key Research and Development Program of China (2023YFD1201000), Local Science and Technology Development Fund Projects of Hebei Province Guided by the Central Government (236Z6501G), the Key R&D Program of Shandong Province (ZR202211070163), Provincial Natural Science Foundation of Hebei (C2022204010), Key Research and Development Project of Shijiazhuang City for University in Hebei Province (241490012A), Hebei Province Dryland Alkali-resistant Wheat Industry Technology System (HBCT2024030206), State Key Laboratory of North China Crop Improvement and Regulation (NCCIR2024ZZ-5), and S&T Program of Hebei (23567601H).

Keywords: GWAS | NADPO | reactive oxygen species | spot blotch | wheat

ABSTRACT

Bipolaris sorokiniana is a prevalent fungal pathogen that resides in the soil and affects various parts of wheat, leading to diseases such as spot blotch, common root rot, head blight and black point. The genetic mechanisms that confer resistance in wheat against this pathogen are not completely known. In this research, 1302 wheat germplasms from around the world were evaluated for resistance to spot blotch at the seedling stage, and it was found that merely 3.8% displayed moderate or better resistance. A genome-wide association study (GWAS) employing high-density 660K single-nucleotide polymorphism (SNP) data pinpointed a segment on chromosome 1BL (621.2–674.0 Mb) containing nine SNPs that are significantly linked to spot blotch resistance, named *Qsb.hebau-1BL*. RNA sequencing and reverse transcription-quantitative PCR analyses demonstrated that the gene *TraesCS1B02G410300*, which codes for nicotinamide-adenine dinucleotide phosphate-binding oxidoreductase (TaNADPO), was markedly upregulated by *B. sorokiniana*. Five SNP variations were identified in the promoter region of *TaNADPO* in wheat lines with or without *Qsb.hebau-1BL*. Wheat lines that overexpressed *TaNADPO* exhibited increased resistance to spot blotch and higher accumulation of reactive oxygen species (ROS). In contrast, knockout EMS mutants of *Triticum turgidum TdNADPO* (*tdnadpo-K2561*, Gln125*) and *TaNADPO* (*tanadpo-J10516796*, splice donor variant) showed diminished resistance and lower ROS levels. In conclusion, *TaNADPO* is a key gene for resistance against *B. sorokiniana*, providing essential information for the development of spot blotch-resistant wheat varieties through molecular breeding techniques.

1 | Introduction

Bipolaris sorokiniana, a fungal pathogen, causes various diseases in wheat and barley, including common root rot, leaf spot blotch, seedling blight, white heads and grain black point. This pathogen presents a serious risk to wheat cultivation and food stability in temperate zones globally, with an increased likelihood of outbreaks in hot and humid climates (Kumar et al. 2002). The

Meng Yuan, Qingdong Zeng,Lei Hua and Shishing Chen contributed equally to this work.

occurrence and intensity of soil-borne diseases in wheat are closely associated with crop rotation practices. Initial studies suggested that multiyear rotations of cereal crops substantially worsen the severity of wheat common root rot due to *B. sorokiniana* (Conner et al. 1996). The extensive adoption of wheat–maize rotation and straw incorporation in northern China has markedly transformed soil organic matter, nutrient levels and nitrogen ratios (Wang et al. 2015; Zhao et al. 2006). This rotation system also affects soil microbial diversity and wheat disease suppression abilities (Peralta et al. 2018). Consequently, the potential damage from *B. sorokiniana* is increasing annually.

Using disease-resistant varieties remains the most economical and effective strategy for controlling wheat diseases caused by *B. sorokiniana*. However, current germplasm resources for *B. sorokiniana*-resistant wheat are limited, and research on the associated genetic resistance loci is still underdeveloped (Roy et al. 2023; Su et al. 2021). Early research incorporated resistance genes for prevalent root rot from wheat relatives such as *Thinopyrum ponticum* (Li et al. 2004). Breeding wheat for resistance to *B. sorokiniana* is significantly challenging due to the governance of resistance by complex quantitative trait loci (QTLs) (Joshi et al. 2004).

Certain QTLs have been discovered through the use of hybrid populations and linkage mapping, including four robust spot blotch (*Sb*) resistance genes. *Sb1* was identified on chromosome 7DS of wheat cultivar Saar, which was tightly linked with *Lr34* and explained 55% of phenotypic variation across six environments (Lillemo et al. 2013). The *Lr34/Yr18/Pm38* gene was found to encode an ATP-binding cassette transporter protein that provides broad-spectrum resistance (Krattinger et al. 2009). *Sb2* was identified from Yangmai 6 on chromosome 5BL linked with the fungal toxin sensitivity gene *Tsn1* and coexists with the powdery mildew resistance gene *PmG25* (Kumar et al. 2015; Kumar et al. 2016). *Sb3* was reported in the winter wheat line 621-7-1, controlled by dominant genes on chromosome 3BS (Lu et al. 2016). *Sb4* was recently identified from the wheat cultivar Zhongyu 1211 and GY17, located on 4BL within a 1.19 cM interval, corresponding to a 1.34 Mb region containing 21 candidate resistance genes (Zhang et al. 2020). Additionally, a minor *Sb* resistance QTL associated with the rust resistance locus *Lr46/Yr29* on chromosome 1BL was detected in the wheat cultivar Saar at the adult plant stage in the field (Lillemo et al. 2013). A recent study has fine-mapped the *Yr29* locus, also known as *QYr.ucw-1BL*, in the Argentinean wheat cultivar Klein Chajá to a region of 0.24 cM and has developed multiple high-throughput markers for it (Cobo et al. 2019).

The sequencing of the wheat genome allows for the application of the 660K high-density SNP gene chip in genome-wide association studies (GWAS) to investigate various QTLs in wheat (Sun et al. 2020). For instance, researchers successfully located the gene *TaDIR-B1* on chromosome 4B by identifying the resistance levels to Fusarium crown rot in 234 Chinese wheat germplasms and conducting GWAS with 660K high-density SNP chip data. This gene negatively regulates the wheat resistance to Fusarium crown rot by modulating the accumulation of lignin in the plant (Yang et al. 2021). In GWAS on wheat common root rot resistance loci, a US research team used a 15K SNP gene chip and 294 wheat accessions to identify 10 pedigrees with strong resistance and six *Sb* resistance QTLs (Ayana et al. 2018). The CIMMYT team used DArTSeq markers for genetic linkage analysis of 301 Afghan wheat varieties resistant to common root rot, finding that about 15% of the Afghan wheat materials had strong resistance, and 25 *Sb* QTL loci were discovered (Bainsla et al. 2020).

This study aimed to identify new wheat resistance germplasms and genetic loci associated with spot blotch caused by *B. sorokiniana*. Through omics analysis, we revealed the molecular mechanisms underlying wheat resistance to spot blotch and explored candidate genes controlling this resistance.

2 | Results

2.1 | A Spot Blotch Resistance Locus, *Qsb.hebau-1BL*, was Identified Through Phenotyping a Large-Scale Collection of Global Common Wheat Germplasms and a GWAS

This collection, which includes 1302 released cultivars, breeding lines and landraces (Figure S1), was subjected to spray inoculation with spores of *B. sorokiniana* at the seedling stage. Spot blotch resistance was assessed employing a disease severity rating (DSR) scale from 0 to 5 (Figure 1a, Table S1). The findings revealed that around 74.8% of the wheat germplasm samples exhibited high DSR ratings (4–5) for spot blotch (Figure 1b), indicating a shortage of resistant materials within the global common wheat germplasm pool. Only about 3.8% of the wheat germplasms with DSR scores < 3.0 were classified as resistant (R) or moderately resistant (MR) (Table S2).

Following the filtering process, 372,277 SNPs were employed in the GWAS to identify QTLs associated with resistance to spot blotch. The GWAS was performed using the univariate mixed linear model (MLM) within the R software environment. A total of 34 highly associated SNPs with $p < 10^{-4}$ were identified (Figure 1c,d, Table S3). Of these, nine SNPs were clustered in a main genomic region on chromosome 1BL. The SNP-located 621.2–674.0 Mb physical interval on chromosome 1BL was designated as *Qsb.hebau-1BL* (Figure 1e). The identified *Qsb.hebau-1BL* was close to a previously reported broad-spectrum resistance QTL to spot blotch, leaf rust and stripe rust (*Qsb/Lr46/Yr29*). There was a total of 40 highly confidently encoded genes within the physical interval of the Chinese Spring reference genome corresponding to *Qsb.hebau-1BL* (Figure 1f, Table S4).

We performed haplotype analysis on the nine SNPs linked to the *Qsb.hebau-1BL* region. By analysing the genotypes of resistant and susceptible wheat germplasms, we identified two main haplotypes, *Qsb(–)* and *Qsb.hebau-1BL*, from these nine SNPs (Table S5). Additionally, we examined the genotype of a key SNP, *AXE-111002968*, within the *Qsb.hebau-1BL* region and found that among 969 accessions, 379 with the *Qsb.hebau-1BL* haplotype had a significantly lower average DSR value compared to the 590 accessions with the *Qsb(–)* haplotype (Figure 1g). Using the SNP data associated with the *Qsb.hebau-1BL* locus, two dCAPS markers were developed to differentiate between wheat genotypes that possess or lack the *Qsb.hebau-1BL* trait (Table S6, Figure S2).

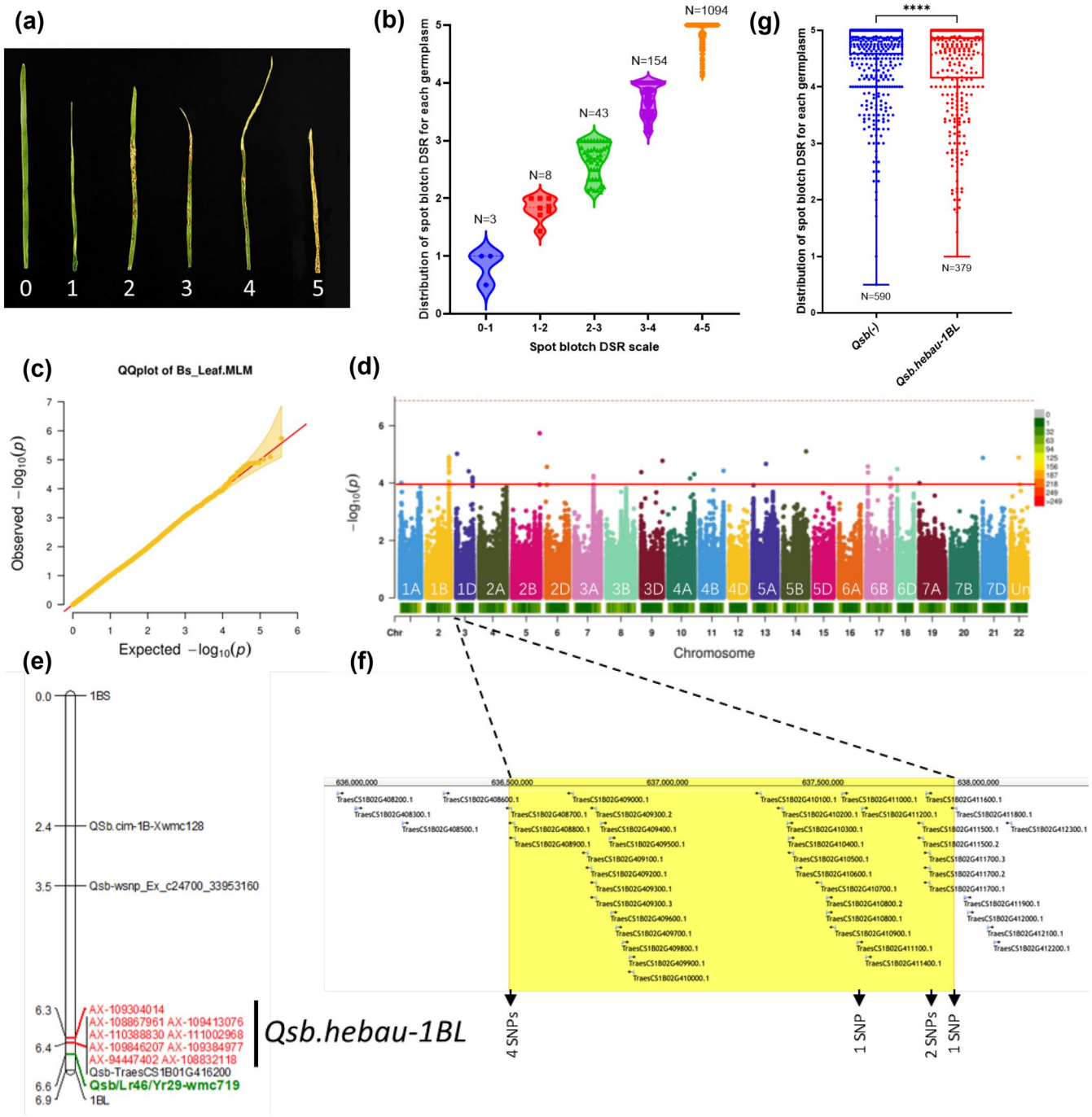

FIGURE 1 | Identification of the genetic locus *Qsb.hebau-1BL* for wheat resistance to spot blotch using genome-wide association study (GWAS). (a) Spot blotch disease severity rating (DSR) in wheat. (b) Distribution of spot blotch DSR among the collected global wheat germplasms. (c) QQ plots for GWAS analysis. (d) Manhattan plot illustrating associations between single-nucleotide polymorphisms (SNPs) and spot blotch resistance identified through GWAS. (e) Distribution map displaying associated SNPs and previously reported spot blotch-resistant quantitative trait loci (QTLs) on chromosome 1B. (f) Physical interval of *Qsb.hebau-1BL* in the Chinese Spring reference genome. (g) Phenotypic effects of wheat germplasms with or without *Qsb.hebau-1BL* on spot blotch resistance. ****$p < 0.0001$, Student's *t* test.

In addition to *Qsb.hebau-1BL*, there were two adjacent SNPs located on chromosome 1DL, two SNPs on chromosome 3AL, two SNPs on chromosome 6BS and three SNPs on chromosome 6BL that were also closely linked to the phenotype of wheat resistance to spot blotch. These were temporarily named *Qsb.hebau-1DL* (462.5–462.9 Mb), *Qsb.hebau-3AL* (541.7–542.2 Mb), *Qsb.hebau-6BS* (51.3–51.9 Mb) and *Qsb.hebau-6BL* (671.0–684.8 Mb), respectively (Figure S3, Table S3).

2.2 | Transcriptome Sequencing Was Initially Used to Explore the Molecular Mechanism of Wheat Resistance to Spot Blotch

Seedlings of three resistant lines R522L_Emai18, R734L_XinXiang9178 and R901L_ZhongYu9398 with *Qsb.hebau-1BL*, and one susceptible line XY22L_Xiaoyan22 without *Qsb.hebau-1BL* were inoculated with either *B. sorokiniana*

(_BS) or water (_CK). A total of 24 RNA samples, comprising three biological replicates for each treatment and genotype pairing, were procured at 48 h post-inoculation (hpi) and underwent 12-Gb Illumina sequencing (Table S7). The transcriptome assembly was conducted using the reference genome of the common wheat variety Chinese Spring version 1.1. The assembly process yielded 143,540 annotated transcripts, with expression levels quantified through FPKM values. Principal component analysis (PCA) of the overall transcript expression profiles revealed that most biological replicates were grouped together (Figure S4). All raw sequencing data have been archived at the NCBI under BioProject accession PRJNA1133090.

Initially, we conducted a comprehensive analysis of the expression patterns of all pathogenesis-related protein (*PR*) gene families within the wheat transcriptome, as depicted in Figure 2a and detailed in Table S8. The majority of these *PR* gene families exhibited significant upregulation in response to *B. sorokiniana* infection in both resistant and susceptible wheat lines, suggesting a widespread activation of plant defence mechanisms against this pathogen. We identified differentially expressed genes (DEGs) across various genotype × treatment combinations, with a $\log_2$-fold change greater than 1 and a *q*-value below 0.05. A Venn diagram was used to illustrate the relationships among these DEGs (Figure 2b). In the susceptible line Xiaoyan22_Qsb(−), *B. sorokiniana* infection resulted in 8506 upregulated and 3274 downregulated DEGs. KEGG pathway analysis for the comparison XY22L_BS vs. XY22L_CK revealed that DEGs were predominantly involved in glutathione metabolism, amino sugar metabolism and phenylalanine metabolism (Figure 2c). In contrast, a total of 2075 upregulated and 1121 downregulated DEGs were identified in the resistant line R522L_Emai18, which carries *Qsb.hebau-1BL*. KEGG pathway analysis for the comparison R522L_BS vs. R522L_CK indicated that DEGs were enriched in pathways related to photosynthesis, phenylpropanoid biosynthesis and the mitogen-activated protein kinase (MAPK) signalling pathway (Figure 2d). Strikingly, within the MAPK signalling pathway, we observed clear activations of the PAMP-triggered immunity (PTI) plant defence response and the abscisic acid (ABA) phytohormone signalling (Figure S5, Table S9).

2.3 | *TaNADPO* was Identified as the Candidate Gene Within the *Qsb.hebau-1BL* Physical Interval

The expression profiles of all 40 annotated genes within the *Qsb.hebau-1BL* physical interval were generated based on the RNA-seq database (Figure 3a, Table S10). In the sequenced RNA samples, the expression of only 14 genes was detected, while others may be pseudogenes with extremely low expression levels. Genomic variations within the *Qsb.hebau-1BL* physical interval were analysed among 10 selected resistant and 10 susceptible wheat lines, with or without *Qsb.hebau-1BL*, using a recent whole-genome resequencing data (Table S11). Among the identified expressed genes, only five exhibited consistent variations between resistant and susceptible haplotypes. Notably, the gene *TraesCS1B02G410300* encoding the nicotinamide-adenine dinucleotide phosphate-binding oxidoreductase known as TaNADPO was significantly upregulated by *B. sorokiniana* across various lines in the transcriptome (Figure 3a). To affirm the expression profile of *TaNADPO* in wheat lines, both resistant (ZhenMai9, harbouring *Qsb.hebau-1BL*) and susceptible (Xiaoyan22, lacking *Qsb.hebau-1BL*) leaf specimens were gathered at 24 and 48 hpi with *B. sorokiniana*. These samples were then analysed using reverse transcription-quantitative PCR (RT-qPCR). The expression level of the *TaNADPO* gene in the wheat line with *Qsb.hebau-1BL* was significantly higher than in the line without *Qsb.hebau-1BL* following *B. sorokiniana* infection at both 24 and 48 hpi (Figure 3b), whereas the other four genes, which also exhibited consistent variations between resistant and susceptible haplotypes, showed no significant alteration in expression levels across different combinations of haplotype and treatment (Figure S6). Based on gene variations and expression patterns, the *TaNADPO* gene was predicted as the functional candidate within the *Qsb.hebau-1BL* locus and was selected for further analysis.

To validate the variations of the *TaNADPO* gene across various lines, the genomic sequence of the *TaNADPO* gene was amplified from 10 lines exhibiting resistance to spot blotch with *Qsb.hebau-1BL* and 10 lines that are susceptible to spot blotch without *Qsb.hebau-1BL* (Table S5). The coding region of the *TaNADPO* gene remains consistent and unchanged across lines, regardless of whether they possess the *Qsb.hebau-1BL* or not. Five SNPs were detected at the −745, −557, −490, −121 and −66 bp positions within the promoter region of the *TaNADPO* gene in wheat lines, irrespective of the presence of the *Qsb.hebau-1BL* allele. These haplotypic variations are located within the binding sites of ABRE-like, RAV1AAT/AP2-like, ARR1, SURECOREATSULTR11 and ACGTATERD1, respectively (Figure 3c, Table S12). Three gene-specific dCAPS markers were developed based on these SNPs (Figure S7, Table S13). We were unable to locate any homologous copies of *TaNADPO* within the A and D subgenomes of common wheat. The encoded TaNADPO protein includes a predicted domain of the NADB_Rossmann superfamily (Figure 3c) and is conserved across various plant species (Figure 3d).

2.4 | The Transient Expression of the *TaNADPO* Gene in *Nicotiana benthamiana* Leaves Significantly Enhanced Plant Resistance to *B. sorokiniana* and the Generation of Reactive Oxygen Species

To ascertain the subcellular distribution of TaNADPO, a green fluorescent protein (GFP) tag was employed to facilitate visualisation of TaNADPO within *N. benthamiana* leaves. Both GFP-TaNADPO and TaNADPO-GFP constructs exhibited cytoplasmic fluorescence in *N. benthamiana* leaves (Figure 4a). To detect the build-up of the reactive oxygen species (ROS) superoxide anions (O^{2-}) in *Agrobacterium*-infiltrated *N. benthamiana* leaves, nitroblue tetrazolium (NBT) was used (Figure 4b). The percentage of the stained area in each fully infiltrated leaf was quantified using Assess software. The results indicated a significantly higher accumulation of O^{2-} in the *TaNADPO*-expressing *N. benthamiana* leaves compared to the GFP control (Figure 4c).

To preliminarily explore the functions of *TaNADPO* in plant defence against *B. sorokiniana*, *TaNADPO* was transiently expressed in *N. benthamiana* leaves, followed by

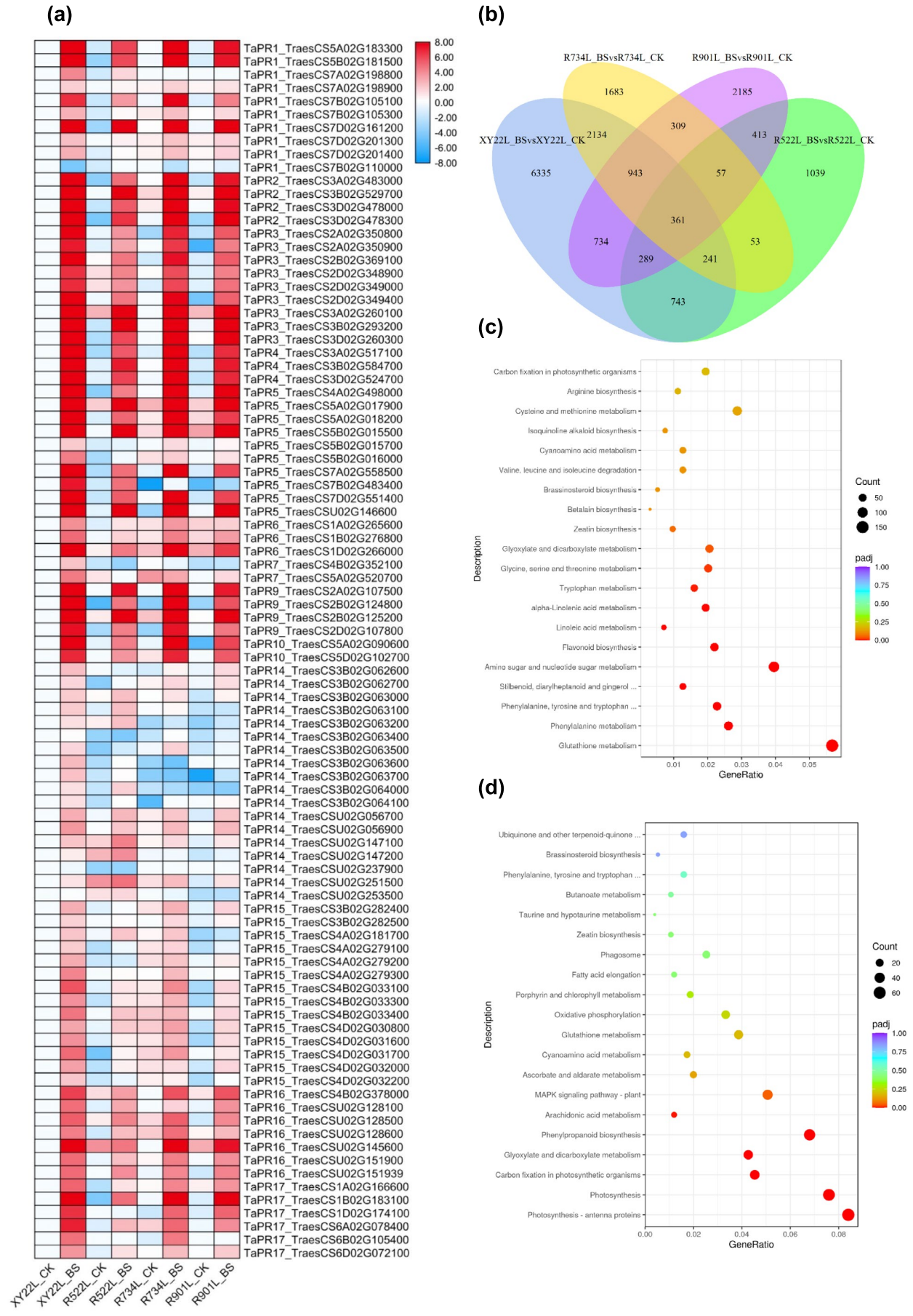

FIGURE 2 | Legend on next page.

FIGURE 2 | Transcriptome sequencing revealed molecular bases of wheat resistance to spot blotch. (a) Expression patterns of *PR* genes in wheat responses to spot blotch. (b) Venn diagrams depicting all differentially expressed genes (DEGs) between each pair of genotype and treatment combinations. (c) Enrichment of KEGG pathways annotated for DEGs in the comparison XY22_Qsb(−)_BS versus XY22_Qsb(−)_CK (inoculated with *Bipolaris sorokiniana* or water, respectively). (d) Enrichment of KEGG pathways annotated for DEGs in the comparison R522_Qsb(+)_BS versus R522_Qsb(+)_CK.

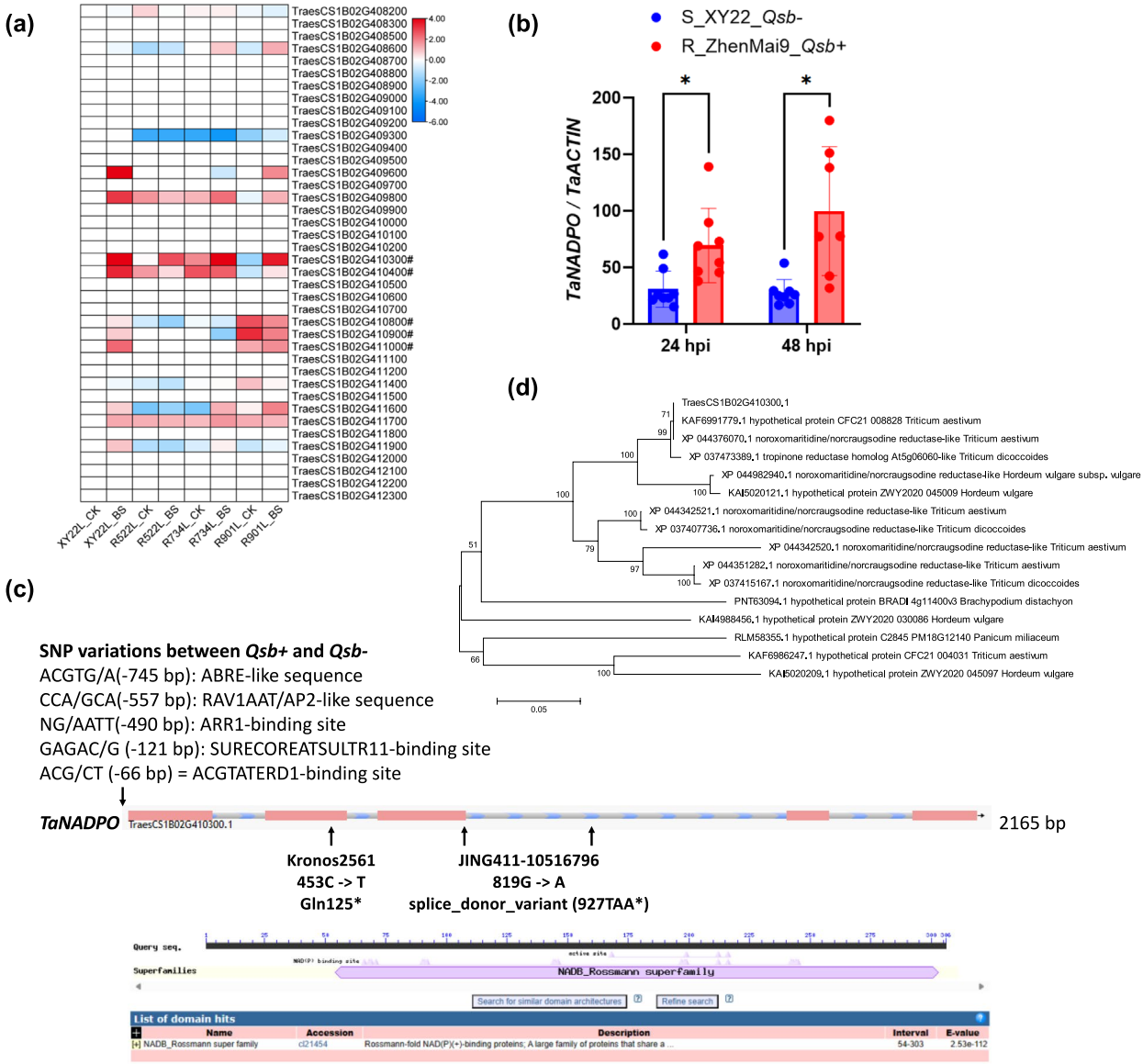

FIGURE 3 | Expression patterns, genomic variations and deduced protein characteristics of the *TaNADPO* gene within the *Qsb.hebau-1BL* locus. (a) Expression patterns of all 40 candidate genes within the *Qsb.hebau-1BL* interval during wheat resistance to spot blotch. (b) Expression levels of *TaNADPO* in wheat lines with *Qsb.hebau-1BL* (ZhenMai 9) and without *Qsb.hebau-1BL* (XY22) upon infection with *Bipolaris sorokiniana*. hpi, hours post-inoculation. *$p < 0.05$, Student's *t* test. (c) Gene structure and single-nucleotide polymorphism (SNP) variations of the *TaNADPO* gene. (d) Phylogenetic tree of TaNADPO protein and its homologues in other plant species.

inoculation with *B. sorokiniana* 2 days after infiltration. Plant cell death was assessed by quantifying the proportion of the trypan blue staining area within the infiltrated leaf region (Figure 4d). Relative to leaves infiltrated with free GFP, the expression of either GFP-TaNADPO or TaNADPO-GFP markedly improved plant resistance to *B. sorokiniana* (Figure 4e).

2.5 | The Transgenic Wheat Line Overexpressing the *TaNADPO* Gene Exhibited Increased Resistance to Spot Blotch due to a Heightened Burst of RO

Transgenic wheat lines with enhanced expression of *TaNADPO* (*TaNADPO-OE*) were developed on the genetic canvas of Fielder,

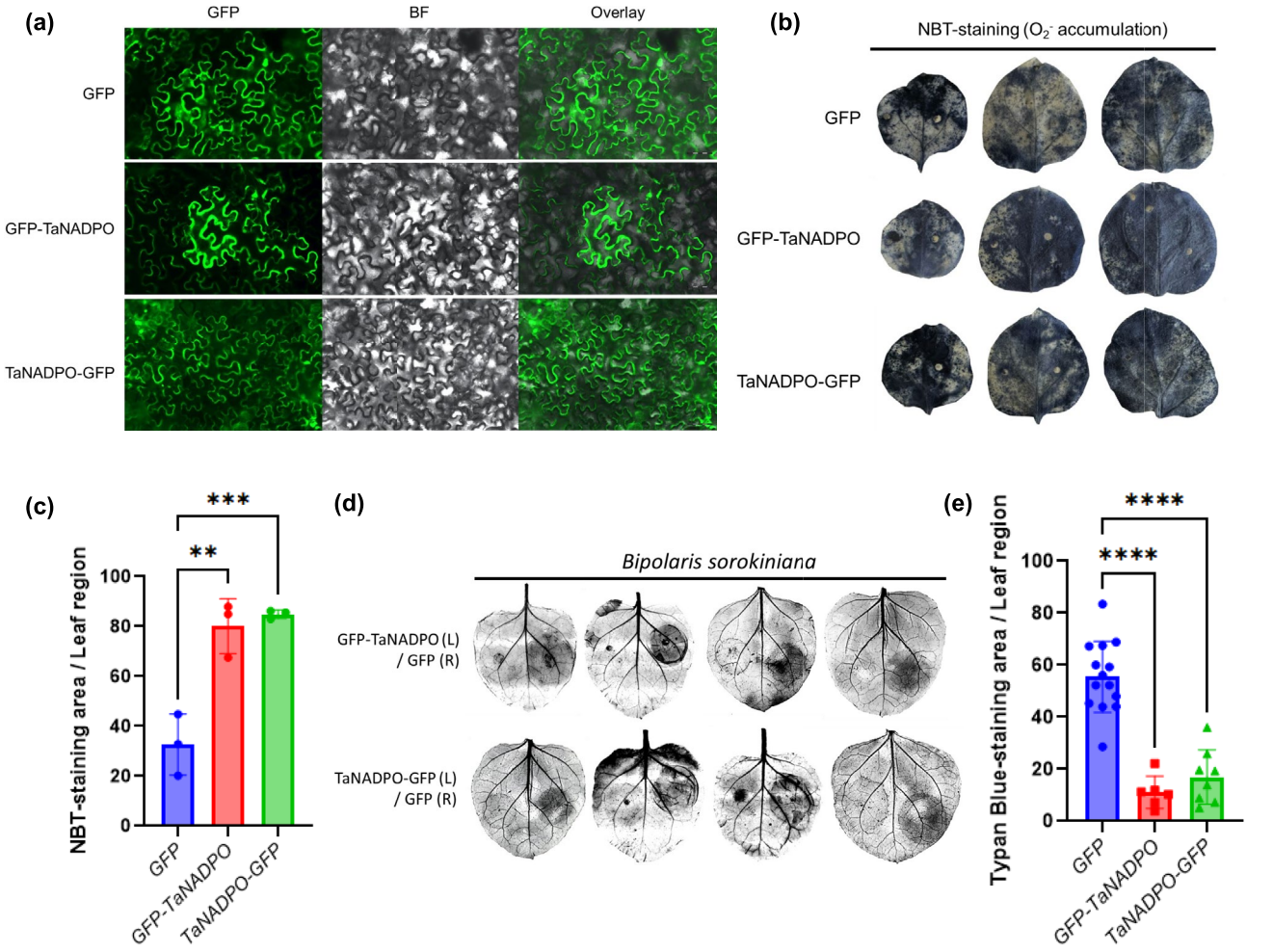

FIGURE 4 | Initial functional characterisation of GFP-labelled TaNADPO in *Nicotiana benthamiana*. (a) Subcellular localisation of GFP-TaNADPO and TaNADPO-GFP transiently expressed in leaves of *N. benthamiana*. Scale bar = 50 μm. (b) Accumulation of reactive oxygen species (ROS) triggered by infiltration of *Agrobacterium tumefaciens* expressing GFP-TaNADPO and TaNADPO-GFP in leaves of *N. benthamiana*. Free GFP was used as a control. (c) Proportions of nitroblue tetrazolium (NBT)-staining areas in the whole leaf region estimated using Assess software and employed for statistical analysis. (d) Infection by *Bipolaris sorokiniana* in the leaf region transiently expressing GFP-TaNADPO and TaNADPO-GFP. Free GFP was used as a control. (e) Proportions of trypan blue-stained cell death areas in the leaf region pre-infiltrated with *A. tumefaciens* carrying *GFP-TaNADPO* and *TaNADPO-GFP*, estimated using Assess software and employed for statistical analysis. $^{**}p < 0.01$, $^{***}p < 0.001$, $^{***}p < 0.0001$, one-way ANOVA.

a variety that is vulnerable to spot blotch (DSR 5.00, Table S1), and devoid of the *Qsb.hebau-1BL* and R-haplotype of *TaNADPO* (Tables S5 and S12). The *TaNADPO* transgene displayed high expression levels across different lines (Figure 5a). The *TaNADPO-OE* transgenic wheat lines exhibited significantly heightened resistance to spot blotch compared to their wild-type counterparts, as illustrated in Figure 5b. Upon inoculation with *B. sorokiniana*, the leaves of wild-type plants exhibited full necrosis at 10 days post-inoculation (dpi), while those of *TaNADPO-OE* only displayed small lesions. The percentage of the spot blotch region in each inoculated leaf was analysed, revealing a significant reduction in *B. sorokiniana* infection in *TaNADPO-OE* (Figure 5c).

Furthermore, the accumulation of O^{2-} induced by *B. sorokiniana* infection at 24 hpi was visualised using NBT staining (Figure 5d). Leaves of *TaNADPO-OE* accumulated a significantly higher amount of O^{2-} upon *B. sorokiniana* infection compared to wild-type plants (Figure 5e).

2.6 | The EMS Knockout Mutants of *nadpo* in Both Tetraploid and Hexaploid Wheat Backgrounds Showed Increased Susceptibility to Spot Blotch, Along With Reduced Accumulation of ROS

In the tetraploid wheat (*Triticum turgidum* subsp. *durum*), the TaNADPO homologue, TdNADPO, exhibited a protein similarity of 99.3% with TaNADPO (as shown in the sequence alignment in Figure S8). The mutant K2561, a stop-gained EMS mutant of *TdNADPO* in the background of tetraploid wheat Kronos, was obtained from a previous exome capture project on durum wheat. Upon genotyping, the wild-type plants of Kronos were found to possess the *Qsb.hebau-1BL* locus and an R-haplotype of *TdNADPO* (Tables S5 and S12). The predicted point mutation of *TdNADPO* at nucleotide position 373, resulting in a CAG to TAG in-frame mutation, leads to the gain of a stop codon, replacing the encoded Gln at position 125. This mutation in the K2561 mutant line was confirmed through PCR

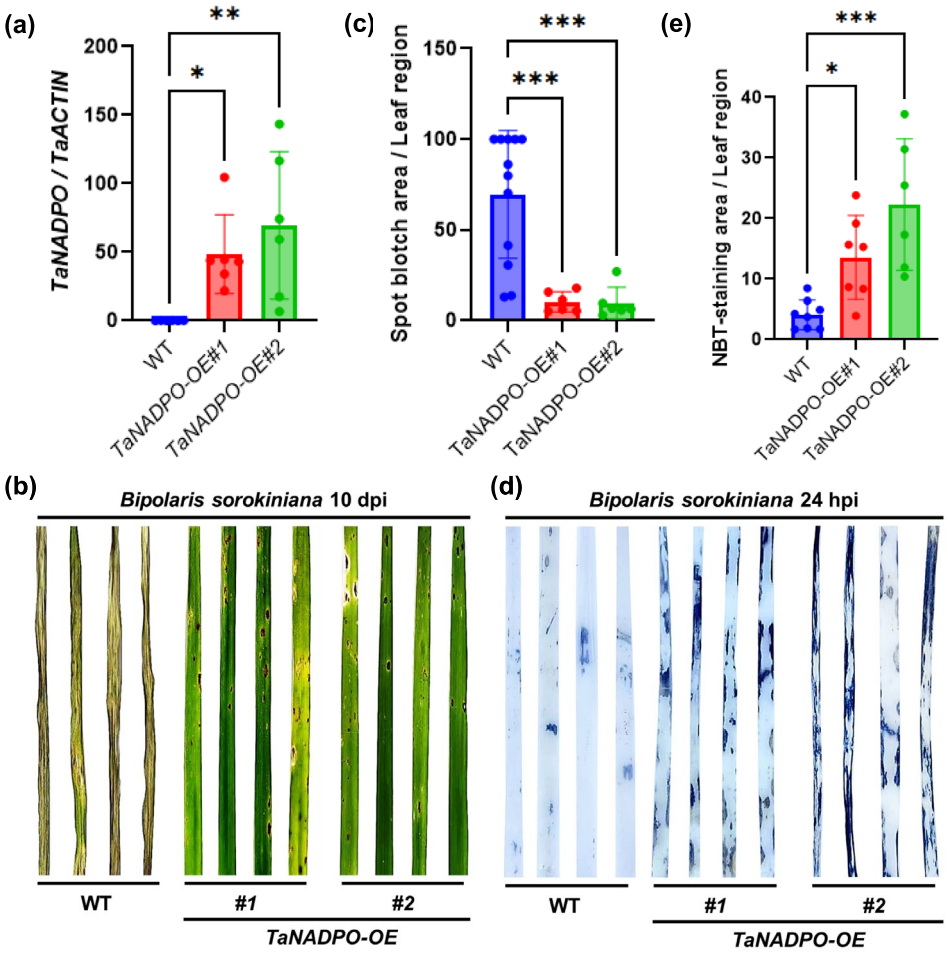

FIGURE 5 | *TaNADPO* promotes wheat resistance to spot blotch with higher accumulation of reactive oxygen species (ROS). (a) Transcript levels of the *TaNADPO* transgene in *TaNADPO-OE*, determined by reverse transcription-quantitative PCR. (b) Phenotypes of *TaNADPO-OE* and wild-type (WT) plants in response to *Bipolaris sorokiniana*. (c) Statistical analysis of the proportion of the spot blotch region on leaves of *TaNADPO-OE* and WT plants. (d) Nitroblue tetrazolium (NBT)-staining of leaves from *TaNADPO-OE* and WT plants inoculated with *B. sorokiniana* at 24 h post-inoculation. (e) Statistical analysis of the proportion of the NBT-staining region on leaves of *TaNADPO-OE* and WT plants infected with *B. sorokiniana*. $^{*}p < 0.05$, $^{**}p < 0.01$, $^{***}p < 0.001$, one-way ANOVA.

amplification and Sanger sequencing (Figure 6a). The mutant line K2561 was back-crossed with wild-type Kronos twice to remove background mutations.

Subsequently, the selected knockout line of *tdnadpo-K2561* and its wild-type Kronos were subjected to spray inoculation with *B. sorokiniana* (Figure 6b). In comparison to the wild-type Kronos, which demonstrated a relatively elevated resistance to spot blotch with a DSR of 2.00 (Table S1), the *tdnadpo-K2561* knockout variant exhibited a markedly diminished resistance to spot blotch (Figure 6c). Furthermore, visualisation of O^{2-} accumulation using NBT staining at 48 hpi revealed that the knockout line *tdnadpo-K2561* exhibited significantly lower levels of ROS production compared to the wild-type plants upon *B. sorokiniana* infection (Figure 6d,e).

A splice donor variant mutation, designated as J10516796, within the *TaNADPO* gene of hexaploid wheat was identified from an exome-sequenced EMS mutant population derived from the cultivar JING411. The wild-type JING411 was also found to have the *Qsb.hebau-1BL* locus and an R-haplotype of *TaNADPO* (Tables S5 and S12). The nucleotide position 819 of *TaNADPO* underwent a predicted point mutation, transitioning from GT to AT, which induced a frameshift mutation and the acquisition of a stop codon TAA at nucleotide position 927. This genetic alteration in the J10516796 mutant line was confirmed through PCR amplification and Sanger sequencing (Figure 7a). To eliminate background mutations, the mutant line J10516796 was back-crossed with the wild-type JING411 on two occasions.

Both the knockout line of *tanadpo-J10516796* and its corresponding wild-type JING411 were subjected to spray inoculation with *B. sorokiniana* (Figure 7b). The wild-type JING411 showed comparatively greater resistance to spot blotch (DSR 2.33, Table S5), whereas the *tanadpo-J10516796* knockout line displayed a significant decrease in resistance to spot blotch disease. Notably, the inoculated leaves of *tanadpo-J10516796* exhibited a significantly higher percentage of lesion areas compared to those seen in the wild-type plants, as depicted in Figure 7c. Additionally, upon infection with *B. sorokiniana*, the knockout line *tanadpo-J10516796* demonstrated substantially lower levels of ROS production compared to the wild-type plants (Figure 7d,e).

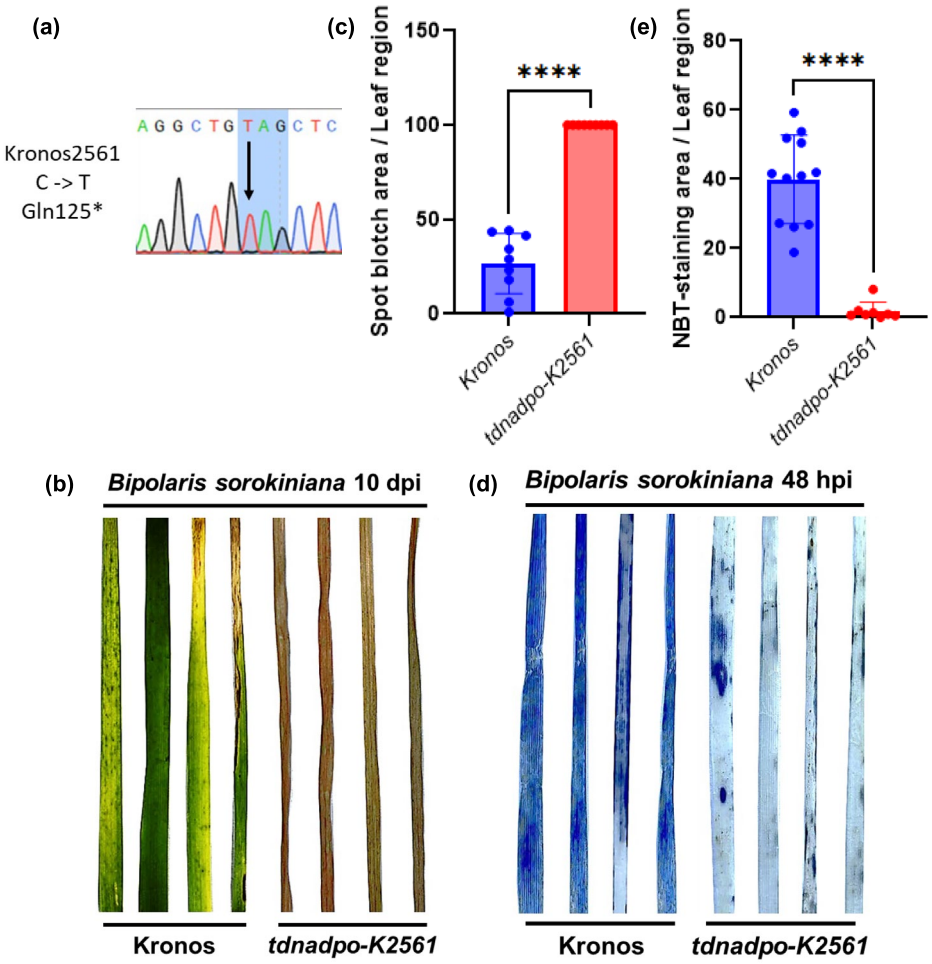

FIGURE 6 | Tetraploid wheat *TdNADPO* knockout mutant showed diminished resistance to spot blotch and attenuated reactive oxygen species (ROS) generation. (a) Sanger sequencing validation of the stop-gained mutation in *TdNADPO* in the Kronos EMS mutant K2561. (b) Phenotypes of *tdnadpo-K2561* and wild-type Kronos plants in response to *Bipolaris sorokiniana*. (c) Statistical analysis of the proportion of the spot blotch region on leaves of *tdnadpo-K2561* and wild-type plants. (d) Nitroblue tetrazolium (NBT)-staining of leaves from *tdnadpo-K2561* and wild-type Kronos plants inoculated with *B. sorokiniana* at 48 h post-inoculation (hpi). (e) Statistical analysis of the proportion of the NBT-staining region on leaves of *tdnadpo-K2561* and wild-type plants infected with *B. sorokiniana*. $p < 0.0001$, Student's *t* test.

3 | Discussion

Bipolaris sorokiniana can infect various organs of the wheat plant throughout its growth stages, leading to spot blotch in leaves, common root rot in stems and roots, white heads in spikes and black points in grains (Al-Sadi 2021). It is noteworthy that *Bipolaris oryzae*, a relative in the same genus causing brown spot disease in rice, poses a significant threat to rice production in India and Bangladesh (Barnwal et al. 2013). Given these concerns, especially in the context of climate change, developing resistance to *B. sorokiniana* is crucial in wheat breeding programmes, particularly in warm and humid regions.

Gupta and colleagues provided a comprehensive overview of the main sources of resistance to spot blotch in the global wheat gene pool (Gupta et al. 2018). Resistance sources against spot blotch appear to be limited. Only approximately 3.8% of collected global wheat germplasms with DSR scores < 3.0 were identified as potential resistance sources in this study. Similarly, a previous investigation into 294 genotypes of hard winter wheat found that only about 5.2% exhibited high resistance (Ayana et al. 2018). These findings underscore the urgent need to explore novel genetic loci that control resistance to spot blotch and integrate newly identified resistance sources into breeding practices.

According to our previous review, as of 2021, a total of 85 genetic loci located across 19 chromosomes of wheat have been identified to regulate plant resistance to *B. sorokiniana* infection (Su et al. 2021). Within these genetic loci, *Sb1* located on chromosome 7DS is associated with the gene *Lr34/Yr18/Pm38*, which confers broad-spectrum resistance. This gene encodes an ATP-binding cassette (ABC) transporter that provides defence against leaf rust, stripe rust and powdery mildew (Krattinger et al. 2009). Other dominant *Sb* genes, namely, *Sb2*, *Sb3* and *Sb4*, have not yet been cloned. In the present study, employing a GWAS approach, nine closely associated SNPs were found to be significantly linked to resistance against spot blotch on chromosome 1BL. The designated genetic locus, *Qsb.hebau-1BL*, is situated in close proximity to a previously identified minor *Sb* resistance QTL linked to the rust resistance locus *Lr46/Yr29* (Lillemo et al. 2013). *Lr46/Yr29*, which governs slow rusting resistance, has not been cloned to date. Although the identified

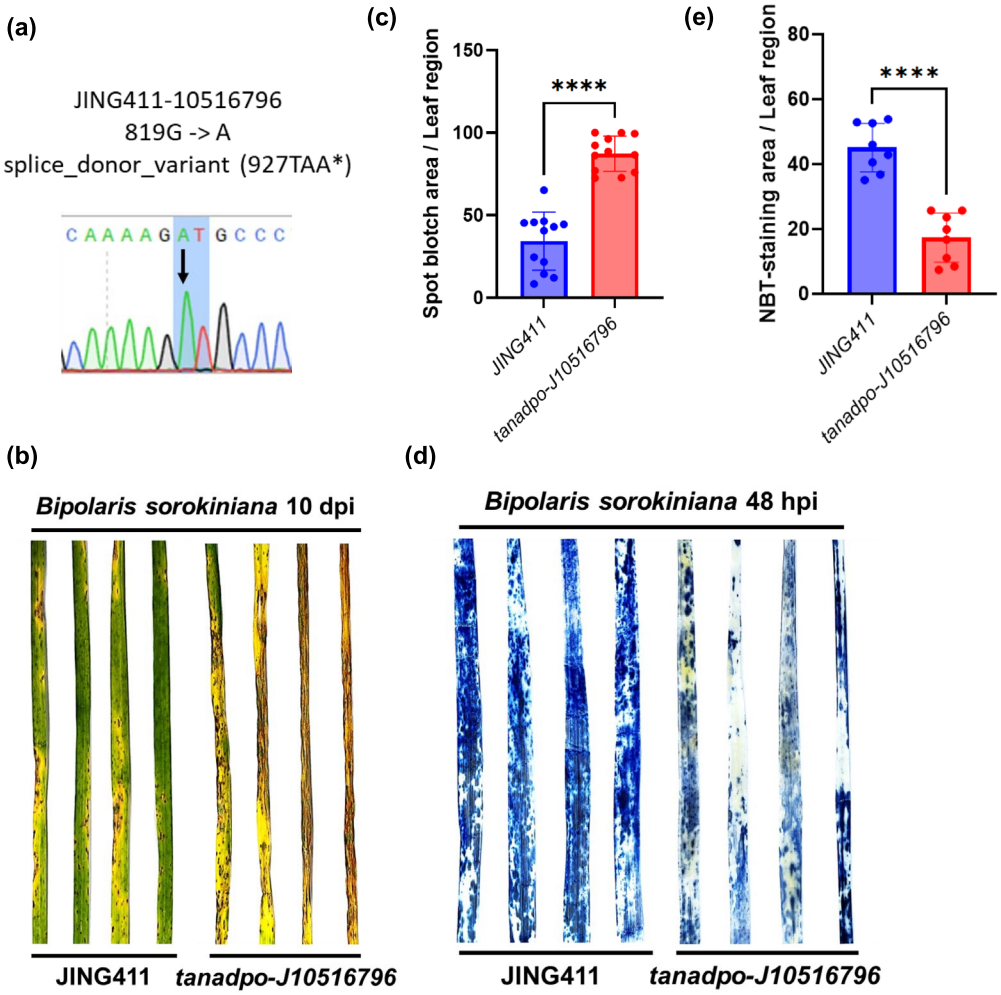

FIGURE 7 | Hexaploid wheat *TaNADPO* knockout mutant showed decreased resistance to spot blotch and reduced reactive oxygen species (ROS) generation. (a) Sanger sequencing validation of the splice donor variant mutation in *TaNADPO* in the JING411 EMS mutant J10516796. (b) Phenotypes of *tanadpo-J10516796* and wild-type JING411 plants in response to *Bipolaris sorokiniana* at 10 days post-inoculation (dpi). (c) Statistical analysis of the proportion of the spot blotch region on leaves of *tanadpo-J10516796* and wild-type plants. (d) Nitroblue tetrazolium (NBT)-staining of leaves from *tanadpo-J10516796* and wild-type plants inoculated with *B. sorokiniana* at 48 h post-inoculation. (e) Statistical analysis of the proportion of the NBT-staining region on leaves of *tanadpo-J10516796* and wild-type plants infected with *B. sorokiniana*. ****$p < 0.0001$, Student's *t* test.

Qsb.hebau-1BL is located near the broad-spectrum disease resistance locus *Lr46/Yr29*, the role of *Qsb.hebau-1BL* and the characterised *TaNADPO* gene in conferring resistance to multiple fungal diseases at the adult plant stage remains to be explored in the future.

While only a limited number of *Sb* genes have been cloned, several transcriptome studies have initially delved into the molecular mechanisms underlying wheat resistance to *B. sorokiniana* infection, encompassing plant responses to spot blotch (Zhang et al. 2022), common root rot (Qalavand et al. 2023) and black point (Li et al. 2021). Our transcriptome analysis revealed that susceptible responses to spot blotch were linked to nutrient metabolism, whereas resistant responses to spot blotch were associated with the activation of *PR* genes, phenylpropanoid biosynthesis and MAPK signalling in the PTI pathway. Like other common necrotrophic pathogens, *B. sorokiniana* probably secretes polygalacturonases (PGs) in the early phases of infection, aiming at the homogalacturonan component of pectin and liberating oligogalacturonides (OGs) with varying chain lengths. These OGs are recognised to elicit classic PTI responses, including a ROS burst, phytoalexin accumulation and hormone biosynthesis (Ghozlan et al. 2020).

The study elucidated the role of the *TaNADPO* gene in plant defence against spot blotch and the regulation of ROS through the use of EMS mutants and transgenic wheat lines. NAD and its phosphorylated counterpart NADP are crucial as energy converters and signalling agents in all living organisms. Within plants, these pyridine nucleotides are integral to various processes, encompassing core energy metabolism, growth and immune responses (Smith et al. 2021). NAD also serves as a key component in plant defence-related signalling and responses, including ROS generation, calcium signalling, DNA repair and protein deacetylation (Pétriacq et al. 2013). In the wheat genome, a total of 46 *NADPO* family genes have been identified, playing widespread roles in plant responses to a broad range of environmental stresses (Hu et al. 2018). However, only a few *TaNADPO* genes have been functionally validated during wheat resistance to phytopathogens.

In conclusion, in a study involving inoculation with *B. sorokiniana*, only 3.8% of the 1302 tested wheat lines showed moderate or higher resistance to spot blotch. A GWAS identified the *Qsb.hebau-1BL* region on chromosome 1BL with significant SNP associations for resistance. The gene *TaNADPO*, which encodes a nicotinamide-adenine dinucleotide phosphate-binding oxidoreductase, was significantly induced in response to *B. sorokiniana* infection. Wheat lines overexpressing *TaNADPO* showed increased resistance and higher ROS accumulation. Conversely, the *nadpo* knockout mutants in both tetraploid and hexaploid wheat had reduced resistance and lower ROS levels. *TaNADPO* plays a pivotal role in conferring resistance to *B. sorokiniana*, offering essential insights for the development of wheat varieties resistant to spot blotch.

4 | Experimental Procedures

4.1 | Wheat Planting and Spot Blotch Inoculation

A highly virulent isolate of *B. sorokiniana* was previously isolated from the field in Baoding, Hebei Province, China (Wei et al. 2021). Spores of *B. sorokiniana* were collected from cultures on potato dextrose agar (PDA) by gently scraping the surface of the culture plate into sterile water. The collected liquid was then filtered using sterile gauze to obtain a spore suspension for inoculation. The concentration of the spore suspension was adjusted to 10^5 spores/mL with the aid of a microscope and a haemocytometer.

A mixture of nutrient soil and vermiculite in a 2:1 ratio was used for growing the wheat seedlings. Ten full-grain seeds of each wheat line were planted in 32-hole trays.

The seedlings of wheat were cultivated in a greenhouse under conditions of 20°C–22°C and a light–dark cycle of 16 h light/8 h dark. Upon reaching the two-leaf stage, the seedlings were subjected to inoculation by thoroughly spraying them with spores of *B. sorokiniana* (approximately 1 mL per plant), after which they were moved to a dark dew chamber maintained at 20°C–22°C with 100% humidity for 48 h. Approximately 10 days post-inoculation (dpi), disease symptoms of spot blotch were recorded for each plant using a DSR scale ranging from 0 to 5:

- Level 0: No disease spots are present on the wheat leaves.
- Level 1: A few scattered disease spots are present, covering approximately 5% of the leaf area.
- Level 2: Disease spots are present, covering about 15% of the leaf area.
- Level 3: Disease spots are prevalent, covering around 30% of the leaf area, with leaf tip necrosis.
- Level 4: Disease spots are extensive, covering roughly 50% of the leaf area, and leaf tip necrosis is evident.
- Level 5: Disease spots are abundant, covering over 70% of the leaf area, or the entire leaf is completely wilted.

The DSR for each wheat line was calculated based on the average of the severity data of each individual plant. Wheat lines underwent two or three independent repetitions of *B. sorokiniana* inoculation, and the final data were obtained by integrating these repetitions to determine the spot blotch resistance phenotype of the entire population.

4.2 | Genotyping and Association Analysis

The 1302 common wheat germplasm resources were genotyped using a 660K high-density SNP chip as described (Wu et al. 2021). In summary, following the acquisition of genotype data, the Affymetrix Genotyping Console (GTC) software was used for preliminary data processing and analysis. SNP loci with a missing genotype rate exceeding 10% were discarded; loci with a minor allele frequency below 5% were eliminated; and loci that did not pass the Hardy–Weinberg equilibrium test at a 1% significance level were omitted. The filtered SNP data were subsequently employed to conduct a GWAS. The polymorphic information content (PIC) was computed to indicate the variability of the SNP loci.

The population structure of 1302 wheat samples was analysed using Structure v. 2.2.3 software, which employs a Bayesian approach. The burn-in parameter was established at 10,000, and the Markov chain Monte Carlo (MCMC) iterations were set to 20,000, with the analysis being conducted five times. The range of subgroup number (K) was from 2 to 10, and the optimal (K) value was determined based on ΔK. The kinship relationships were represented by a kinship heatmap drawn using R (Figure S9).

Whole genome and subgenome linkage disequilibrium (LD) analysis was performed using PLINK software. After SNP data processing, LD was computed using R^2 as the reference standard for pairwise markers. The step-shift window was set to 1000 kb, and the sliding window was set to 30,000 kb. When drawing the distance decay LOESS curve, the genome LD decay distance standard was the marker interval when $R^2 \leq 0.1$. The decay graph for LD in the wheat genome encompassed the LD decay distances for both the entire wheat genome and the ABD subgenomes (Figure S10). High-confidence loci within the same chromosome LD decay distance were considered the same QTL locus.

Using a univariate MLM, R software was employed to perform association analysis of the spot blotch phenotypic data of the 1302 wheat lines with 660K high-density SNP genotype data. GEC software calculated the p-value range for each chromosome, and 10^{-4} was regarded as the threshold for significant loci based on the association analysis results. The results were visualised using R's QQman package to draw Manhattan plots and QQ plots. Additionally, GCTA software was used to calculate the genetic contribution of loci on chromosomes.

4.3 | Genetic Loci Analysis and dCAPS Marker Design

The positions of SNPs and nearby genes with significant associations were analysed using the Chinese Spring reference genome for wheat (v. 1.1). The genetic loci discovered in this

research were charted onto chromosomes with the aid of MapChart v. 2.32 software and contrasted with previously documented loci on the same chromosome (Su et al. 2021). Haplotype analysis was conducted on the grouped significant SNPs, succeeded by an analysis of the phenotypic effects grounded in the haplotype and phenotype data from the GWAS population.

Based on the results of the GWAS, SNPs in close linkage with *Qsb.hebau-1BL* were chosen to create derived cleaved amplified polymorphic sequence (dCAPS) markers (Table S6) following the method described (Neff et al. 1998). The NEBcutter tool v. 2.0 (http://www.labtools.us/nebcutter-v2-0/) was used to pinpoint potential restriction sites for each SNP. Genome-specific primers were crafted using the Primer 3 website (https://bioinfo.ut.ee/primer3-0.4.0/primer3/) to target regions surrounding the SNPs of interest. The PCR products were sequenced to confirm the presence of SNPs. Subsequently, the amplified PCR products were subjected to digestion with specific restriction enzymes. The reliability of molecular markers was evaluated by examining the correlation between the detected genotypic signals and the phenotypes for disease resistance.

4.4 | RNA-Sequencing and Bioinformatic Analysis

Seedlings of selected wheat lines resistant to *B. sorokiniana*, namely, R522 (EMai 18), R734 (XinXiang 9178) and R901 (ZhongYu 9398), along with susceptible control XY22 (XiaoYan 22), were spray-inoculated with *B. sorokiniana* spores as described previously. Sterile water was used as a mock inoculation control (CK). At 5 dpi, leaf samples were collected and sent to Novogene Corporation Ltd for RNA sequencing. Three biological replicates were prepared for each genotype × treatment combination, and the RNA samples were sequenced using the Illumina HiSeq 1000 System with a target output of 12 Gb per sample. The assembly of the transcriptome was conducted employing the Hisat2 v. 2.2.1 software (Kim et al. 2019), using the reference genome for the wheat cultivar Chinese Spring v. 1.1. Gene expression levels were estimated using the StringTie v. 1.3.3b software (Pertea et al. 2015) based on the expected number of fragments per kilobase of transcript sequence per million base pairs (FPKM). Expression of *PR* genes was determined based on gene accessions provided in an early investigation (Zhao et al. 2024). Heatmaps based on FPKM values were created using TBtools v. 1.108 software (Chen et al. 2020). DEGs were identified through the use of DESeq2 v. 1.22.1 software (Love et al. 2014) and were annotated using Gene Ontology (GO) (Young et al. 2010) and the Kyoto Encyclopedia of Genes and Genomes (KEGG) (Kanehisa et al. 2007).

4.5 | Expression and Variations of the *TaNADPO* Gene

Seedlings of the wheat resistance line ZhenMai 9, which carries *Qsb.hebau-1BL*, and the susceptible line XiaoYan 22, which lacks *Qsb.hebau-1BL*, were spray-inoculated with *B. sorokiniana* spores as described previously. Leaf samples were taken from plants 24 and 48 hpi for analysis. RNA was isolated using an RNA Extraction Kit (Qiagen) and cDNA was produced using a Reverse Transcription Kit (TaKaRa). Primers for the RT-qPCR targeting the *TaNADPO* gene were specifically designed (Table S13). The *TaACTIN* gene from wheat (GenBank accession number AB181991) served as an internal control (Paolacci et al. 2009). The transcript levels were expressed relative to *TaACTIN* using the $2^{-\Delta Ct}$ method as described (Li et al. 2023). Data analysis and multiple unpaired *t* tests were conducted using Prism software v. 10.0 (Table S14).

The genomic region of the *TaNADPO* gene was amplified from 10 resistant lines carrying *Qsb.hebau-1BL* and 10 susceptible lines lacking *Qsb.hebau-1BL* (Table S5). The DNA, after amplification, underwent Sanger sequencing to identify variations in the promoter region of the *TaNADPO* gene. Gene-specific dCAPS markers for the *TaNADPO* gene were developed using these SNPs (Table S4).

Homologous sequences for the wheat TaNADPO protein were retrieved from the reference genomes of wheat and its wild relatives available at https://wheat.pw.usda.gov/blast/, as well as from the NCBI database (https://www.ncbi.nlm.nih.gov). Multiple sequence alignment was conducted using the MUSCLE algorithm implemented in MEGA software v. 7.0. The phylogenetic tree was constructed using the pairwise deletion option with bootstrapping at 1000 iterations and was visualised with the help of Interactive Tree of Life (iTOL) v. 5.0 (https://itol.embl.de/). The conserved domain of the TaNADPO protein was predicted through the NCBI Conserved Domain Search at https://www.ncbi.nlm.nih.gov/Structure/cdd/wrpsb.cgi.

4.6 | Gene Expression in *N. benthamiana* Leaves

The full-length TaNADPO protein-coding regions were cloned into both the pGWB5 (35S::*gene-GFP*) and pMDC43 (35S::*GFP-gene*) vectors. These constructs were then expressed in *N. benthamiana* leaves via transformation with *Agrobacterium tumefaciens* GV3101. Fluorescence was observed at 48 hpi using a Nikon Ti-2 microscope.

During staining for ROS, leaves that had been infiltrated with *A. tumefaciens* were harvested at 1 day post-infiltration (dpi) and subsequently treated with nitroblue tetrazolium (NBT) to enable the visualisation of superoxide anion (O^{2-}) accumulation, as per the method described (Zhao et al. 2020). In summary, leaves were gathered and submerged in a solution with 10 mM NaN_3 and 10 mM potassium phosphate buffer (pH 7.8) supplemented with 0.1% NBT (wt/vol) for 24 h. Subsequently, the samples were decolorised using boiling 95% ethanol for 10 min. The stained area percentage for each leaf was calculated with Assess v. 2.0 software (Lamari 2008), and statistical analysis was conducted using one-way ANOVA with Prism software v. 10.0.

For the *B. sorokiniana* inoculation assay, 2 dpi with transformed *A. tumefaciens*, the inoculation solution of *B. sorokiniana* spores was infiltrated into the same area as described (Wang et al. 2024). Approximately 3 days later, disease lesions/necrosis induced by *B. sorokiniana* on *N. benthamiana* leaves were observed and evaluated using Assess v. 2.0 software.

4.7 | Wheat Transgenic Line Overexpressing *TaNADPO*

The transgenic wheat lines used in this research were produced by Jinan Bangdi Ltd Company in Shandong, China, using the spring wheat variety Fielder as the genetic base. To develop the transgenic wheat line *TaNADPO-OE*, the complete open reading frame (ORF) of *TaNADPO* was inserted into the pLGY-02 (Ubi::*gene*, T-DNA) vector (Qin et al. 2023). *Agrobacterium*-mediated transformation was employed to generate the transgenic lines. Initial validation of transgenic lines was performed by PCR amplification of the transgene insertion in genomic DNA using specific primers (Table S2). The levels of *TaNADPO* transgene expression in the transgenic wheat lines were assessed via RT-qPCR analysis. Data were subjected to statistical evaluation using one-way ANOVA with Prism software v. 10.0. Inoculation of *B. sorokiniana* and ROS staining assays were conducted as described above. The inoculation of *B. sorokiniana* and subsequent staining of ROS at 24 hpi were performed as previously described. The experiment comprised two separate transgenic lines, each containing 6–10 biological replicates. Statistical analysis was performed using Prism software v. 10.0, and one-way ANOVA was conducted to determine significant differences.

4.8 | EMS Mutants of Tetraploid Wheat *TdNADPO* and Hexaploid Wheat *TaNADPO* Knockout Lines

The homologue of *TaNADPO* in tetraploid wheat (*TdNADPO*) was identified using annotations in the JBrowse database for wheat genomes available on the WheatOmics database (http://wheatomics.sdau.edu.cn/jbrowse.html). The protein sequences of TaNADPO and TdNADPO were aligned using MEGA software v. 7.0. A stop-gained EMS mutant of the *TdNADPO* gene was predicted from a previous exome capture project on Kronos (Krasileva et al. 2017). This mutant line, K2561, was obtained from the publicly released seed library at Shandong Agricultural University, China. The genomic region containing the predicted mutation at 373 nucleotides from the initiation codon of the *TdNADPO* gene was amplified from both K2561 and wild-type Kronos plants. The amplified DNA was sequenced using Sanger sequencing. The mutant line K2561 was backcrossed twice with wild-type Kronos to eliminate background mutations. The knockout line *tdnadpo-K2561* was selected from the purified BC_2F_1 progeny.

A splice donor variant mutation of the hexaploid wheat *TaNADPO* gene has been discovered within the sequenced exome of the JING411 EMS mutant populations (Xiong et al. 2023). This particular mutant line, designated as J10516796, was sourced from MolBreeding Ltd., located in China. A genomic segment encompassing the predicted mutation, positioned 819 nucleotides downstream from the initiation codon of the *TaNADPO* gene, was amplified from both the mutant line J10516796 and the wild-type JING411 plants. Sanger sequencing was employed to sequence the amplified DNA. To eliminate potential background mutations, the mutant line J10516796 was subjected to two rounds of backcrossing with the wild-type JING411. Subsequently, the knockout line, designated as *tanadpo-J10516796*, was selected from the purified BC_2F_1 progeny.

Seedlings from the *tdnadpo-K2561* and *tanadpo-J10516796* knockout lines, as well as from their respective wild-type plants, were subjected to spray inoculation with *B. sorokiniana* and subsequently stained with NBT at 48 hpi, as previously detailed. Each line was represented by 6–10 biological replicates. Statistical analysis was conducted using Prism software v. 10.0, and an unpaired *t* test was employed to ascertain significant differences.

Acknowledgements

Work at the X.W. laboratory was supported by the National Key Research and Development Program of China (2023YFD1201002), Local Science and Technology Development Fund Projects of Hebei Province guided by the Central Government (236Z6501G), Provincial Natural Science Foundation of Hebei (C2022204010), Key Research and Development Project of Shijiazhuang City for University in Hebei Province (241490012A), Hebei Province Dryland Alkali-Resistant Wheat Industry Technology System (HBCT2024030206), State Key Laboratory of North China Crop Improvement and Regulation (NCCIR2024ZZ-5) and S&T Program of Hebei (23567601H). Work at the S.C. laboratory was supported by the Key R&D Program of Shandong Province (ZR202211070163).

Conflicts of Interest

The authors declare no conflicts of interest.

Data Availability Statement

The sequence data that support the finding of this study are available in the NCBI Sequence Read Archive database at https://www.ncbi.nlm.nih.gov/sra with the accession no. PRJNA1133090. Other data that support the findings of this study are available from the corresponding author upon reasonable request.

References

Al-Sadi, A. M. 2021. "*Bipolaris sorokiniana*-Induced Black Point, Common Root Rot, and Spot Blotch Diseases of Wheat: A Review." *Frontiers in Cellular and Infection Microbiology* 11: 584899.

Ayana, G. T., S. Ali, J. S. Sidhu, J. L. G. Hernandez, B. Turnipseed, and S. K. Sehgal. 2018. "Genome-Wide Association Study for Spot Blotch Resistance in Hard Winter Wheat." *Frontiers in Plant Science* 9: 926.

Bainsla, N. K., R. M. Phuke, X. He, et al. 2020. "Genome-Wide Association Study for Spot Blotch Resistance in Afghan Wheat Germplasm." *Plant Pathology* 69: 1161–1171.

Barnwal, M. K., A. Kotasthane, N. Magculia, et al. 2013. "A Review on Crop Losses, Epidemiology and Disease Management of Rice Brown Spot to Identify Research Priorities and Knowledge Gaps." *European Journal of Plant Pathology* 136: 443–457.

Chen, C., H. Chen, Y. Zhang, et al. 2020. "TBtools: An Integrative Toolkit Developed for Interactive Analyses of Big Biological Data." *Molecular Plant* 13: 1194–1202.

Cobo, N., H. Wanjugi, E. Lagudah, and J. Dubcovsky. 2019. "A High-Resolution Map of Wheat *QYr.Ucw-1BL*, an Adult Plant Stripe Rust Resistance Locus in the Same Chromosomal Region as *Yr29*." *Plant Genome* 12, no. 1: 180055.

Conner, R. L., L. J. Duczek, G. C. Kozub, and A. D. Kuzyk. 1996. "Influence of Crop Rotation on Common Root Rot of Wheat and Barley." *Canadian Journal of Plant Pathology* 18: 247–254.

Ghozlan, M. H., E.-A. Eman, S. Tokgöz, D. K. Lakshman, and A. Mitra. 2020. "Plant Defense Against Necrotrophic Pathogens." *American Journal of Plant Sciences* 11: 2122–2138.

Gupta, P., R. Chand, N. Vasistha, et al. 2018. "Spot Blotch Disease of Wheat: The Current Status of Research on Genetics and Breeding." *Plant Pathology* 67: 508–531.

Hu, C.-H., X.-Y. Wei, B. Yuan, et al. 2018. "Genome-Wide Identification and Functional Analysis of *NADPH Oxidase* Family Genes in Wheat During Development and Environmental Stress Responses." *Frontiers in Plant Science* 9: 906.

Joshi, A. K., S. Kumar, R. Chand, and G. Ortizferrara. 2004. "Inheritance of Resistance to Spot Blotch Caused by *Bipolaris sorokiniana* in Spring Wheat." *Plant Breeding* 123: 213–219.

Kanehisa, M., M. Araki, S. Goto, et al. 2007. "KEGG for Linking Genomes to Life and the Environment." *Nucleic Acids Research* 36: D480–D484.

Kim, D., J. M. Paggi, C. Park, C. Bennett, and S. L. Salzberg. 2019. "Graph-Based Genome Alignment and Genotyping With HISAT2 and HISAT-Genotype." *Nature Biotechnology* 37: 907–915.

Krasileva, K. V., H. A. Vasquez-Gross, T. Howell, et al. 2017. "Uncovering Hidden Variation in Polyploid Wheat." *Proceedings of the National Academy of Sciences of the United States of America* 114: E913–E921.

Krattinger, S. G., E. S. Lagudah, W. Spielmeyer, et al. 2009. "A Putative ABC Transporter Confers Durable Resistance to Multiple Fungal Pathogens in Wheat." *Science* 323: 1360–1363.

Kumar, J., P. Schafer, R. Huckelhoven, et al. 2002. "*Bipolaris sorokiniana*, a Cereal Pathogen of Global Concern: Cytological and Molecular Approaches Towards Better Control." *Molecular Plant Pathology* 3: 185–195.

Kumar, S., M. S. Röder, R. P. Singh, et al. 2016. "Mapping of Spot Blotch Disease Resistance Using NDVI as a Substitute to Visual Observation in Wheat (*Triticum aestivum* L.)." *Molecular Breeding* 36: 95.

Kumar, S., M. S. Roder, S. B. Tripathi, et al. 2015. "Mendelization and Fine Mapping of a Bread Wheat Spot Blotch Disease Resistance QTL." *Molecular Breeding* 35: 218.

Lamari, L. 2008. *Assess 2.0: Image Analysis Software for Plant Disease Quantification*. APS Press.

Li, H., R. L. Conner, Q. Chen, et al. 2004. "The Transfer and Characterization of Resistance to Common Root Rot From *Thinopyrum ponticum* to Wheat." *Genome* 47: 215–223.

Li, H., L. Hua, S. Zhao, et al. 2023. "Cloning of the Wheat Leaf Rust Resistance Gene *Lr47* Introgressed From *Aegilops speltoides*." *Nature Communications* 14: 6072.

Li, Q., C. Gao, K. Xu, et al. 2021. "Transcriptome-Based Analysis of Resistance Mechanism to Black Point Caused by *Bipolaris sorokiniana* in Wheat." *Scientific Reports* 11: 6911.

Lillemo, M., A. K. Joshi, R. Prasad, R. Chand, and R. P. Singh. 2013. "QTL for Spot Blotch Resistance in Bread Wheat Line Saar Co-Locate to the Biotrophic Disease Resistance Loci *Lr34* and *Lr46*." *Theoretical and Applied Genetics* 126: 711–719.

Love, M. I., W. Huber, and S. Anders. 2014. "Moderated Estimation of Fold Change and Dispersion for RNA-Seq Data With DESeq2." *Genome Biology* 15: 1–21.

Lu, P., Y. Liang, D. F. Li, et al. 2016. "Fine Genetic Mapping of Spot Blotch Resistance Gene *Sb3* in Wheat (*Triticum aestivum*)." *Theoretical and Applied Genetics* 129, no. 3: 577–589.

Neff, M. M., J. D. Neff, J. Chory, and A. E. Pepper. 1998. "dCAPS, a Simple Technique for the Genetic Analysis of Single Nucleotide Polymorphisms: Experimental Applications in *Arabidopsis thaliana* Genetics." *Plant Journal* 14: 387–392.

Paolacci, A. R., O. A. Tanzarella, E. Porceddu, and M. Ciaffi. 2009. "Identification and Validation of Reference Genes for Quantitative RT-PCR Normalization in Wheat." *BMC Molecular Biology* 10: 1–27.

Peralta, A. L., Y. Sun, M. D. McDaniel, and J. T. Lennon. 2018. "Crop Rotational Diversity Increases Disease Suppressive Capacity of Soil Microbiomes." *Ecosphere* 9: e02235.

Pertea, M., G. M. Pertea, C. M. Antonescu, T.-C. Chang, J. T. Mendell, and S. L. Salzberg. 2015. "StringTie Enables Improved Reconstruction of a Transcriptome From RNA-Seq Reads." *Nature Biotechnology* 33: 290–295.

Pétriacq, P., L. de Bont, G. Tcherkez, and B. Gakière. 2013. "NAD: Not Just a Pawn on the Board of Plant–Pathogen Interactions." *Plant Signaling & Behavior* 8: e22477.

Qalavand, F., M. Nasr-Esfahani, J. Vatandoost, and D. A. Azarm. 2023. "Transcriptome-Based Analysis of Resistance Mechanisms to *Bipolaris sorokiniana*, a Common Wheat Root-Rot Disease." *Plant Biology* 25: 119–130.

Qin, Y.-x., B. Zhang, S.-f. Cui, X.-c. Qin, and G.-y. Li. 2023. "TaFLZ54D Enhanced Salt Stress Tolerance of Wheat by Interacting With TaSGT1a and TaPP2Ca." *Journal of Integrative Agriculture* 24: 1017–1029.

Roy, C., X. He, N. C. Gahtyari, S. Mahapatra, and P. K. Singh. 2023. "Managing Spot Blotch Disease in Wheat: Conventional to Molecular Aspects." *Frontiers in Plant Science* 14: 401.

Smith, E. N., M. Schwarzländer, R. G. Ratcliffe, and N. J. Kruger. 2021. "Shining a Light on NAD- and NADP-Based Metabolism in Plants." *Trends in Plant Science* 26: 1072–1086.

Su, J., J. Zhao, S. Zhao, et al. 2021. "Genetics of Resistance to Common Root Rot (Spot Blotch), *Fusarium* Crown Rot, and Sharp Eyespot in Wheat." *Frontiers in Genetics* 12: 699342.

Sun, C., Z. Dong, L. Zhao, Y. Ren, N. Zhang, and F. Chen. 2020. "The Wheat 660K SNP Array Demonstrates Great Potential for Marker-Assisted Selection in Polyploid Wheat." *Plant Biotechnology Journal* 18: 1354–1360.

Wang, C., M. Sun, P. Zhang, et al. 2024. "Genome-Wide Association Studies on Chinese Wheat Cultivars Reveal a Novel *Fusarium* Crown Rot Resistance Quantitative Trait Locus on Chromosome 3BL." *Plants* 13: 856.

Wang, J., X. Wang, M. Xu, et al. 2015. "Contributions of Wheat and Maize Residues to Soil Organic Carbon Under Long-Term Rotation in North China." *Scientific Reports* 5: 11409.

Wei, X., Z. Xu, N. Zhang, W. Yang, D. Liu, and L. Ma. 2021. "Synergistic Action of Commercially Available Fungicides for Protecting Wheat From Common Root Rot Caused by *Bipolaris sorokiniana* in China." *Plant Disease* 105: 667–674.

Wu, J., R. Yu, H. Wang, et al. 2021. "A Large-Scale Genomic Association Analysis Identifies the Candidate Causal Genes Conferring Stripe Rust Resistance Under Multiple Field Environments." *Plant Biotechnology Journal* 19: 177–191.

Xiong, H., H. Guo, M. Fu, et al. 2023. "A Large-Scale Whole-Exome Sequencing Mutant Resource for Functional Genomics in Wheat." *Plant Biotechnology Journal* 21: 2047–2056.

Yang, X., S. Zhong, Q. Zhang, Y. Ren, C. Sun, and F. Chen. 2021. "A Loss-Of-Function of the Dirigent Gene *TaDIR-B1* Improves Resistance to *Fusarium* Crown Rot in Wheat." *Plant Biotechnology Journal* 19: 866–868.

Young, M. D., M. J. Wakefield, G. K. Smyth, and A. Oshlack. 2010. "Gene Ontology Analysis for RNA-Seq: Accounting for Selection Bias." *Genome Biology* 11: 1–12.

Zhang, P., G. Guo, Q. Wu, et al. 2020. "Identification and Fine Mapping of Spot Blotch (*Bipolaris sorokiniana*) Resistance Gene *Sb4* in Wheat." *Theoretical and Applied Genetics* 133: 2451–2459.

Zhang, X., T. Huang, Q. Wang, et al. 2022. "Mechanisms of Resistance to Spot Blotch in Yunnan Iron Shell Wheat Based on Metabolome and Transcriptomics." *International Journal of Molecular Sciences* 23: 5184.

Zhao, R., X. Chen, F. Zhang, H. Zhang, J. L. Schroder, and V. Romheld. 2006. "Fertilization and Nitrogen Balance in a Wheat–Maize Rotation System in North China." *Agronomy Journal* 98: 938–945.

Zhao, S., M. Li, X. Ren, et al. 2024. "Enhancement of Broad-Spectrum Disease Resistance in Wheat Through Key Genes Involved in Systemic Acquired Resistance." *Frontiers in Plant Science* 15: 1355178.

Zhao, S., X. Shang, W. Bi, et al. 2020. "Genome-Wide Identification of Effector Candidates With Conserved Motifs From the Wheat Leaf Rust Fungus *Puccinia triticina*." *Frontiers in Microbiology* 11: 1188.

Supporting Information

Additional supporting information can be found online in the Supporting Information section.